The Term Structure of Macroeconomic Risks at the Effective Lower Bound

Guillaume ROUSSELLET*

November 2022

Abstract

This paper proposes a new macro-finance model that solves the tension between tractability, flexibility in macroeconomic dynamics, and consistency of the term structures of treasury yields with the effective lower bound (ELB). I use the term structures of U.S. nominal and real treasury yields from 1990 to explore the interdependence between inflation expectations, volatility, and monetary policy at the ELB. The estimation reveals that real yields stay elevated during the ELB due to large premia and deflation fears, produced by a persistent shift in inflation dynamics, with low average inflation and heightened inflation volatility.

JEL Codes: C58, E43, G12

Key-words: Affine Term Structure Model, Effective Lower Bound, TIPS, Liftoff Probabilities, Inflation Risk Premia.

*McGill University – Desautels School of Management, 1001 Sherbrooke St. West, Montreal QC H3A 1G5, CANADA, guillaume.roussellet@mcgill.ca

1 Introduction

During the last decade, U.S. short-term interest rates have shown an unprecedented behavior being stuck at their effective lower bound (ELB henceforth) for an exceptionally long period. As conventional monetary policy easing becomes unfeasible, questions emerge on the central bank's ability to escape the deflation trap and stimulate the economy. At the heart of this debate is the idea that the ELB is a fundamentally different state of the world where the relationship between interest rates and macroeconomic outcomes cannot be understood using pre-ELB data (see e.g., the discussion between Cochrane (2017) and Christiano (2017)). Models adapted to pre- and post-ELB periods are therefore central for monetary policymakers, as they are key to understand if real yields are elevated because of prolonged expected deflation, large risk premia, or both, and provide the appropriate policy action.

While existing macro-finance models can guide these policy questions, they must address conflicting challenges. On the one hand, traditional *affine* and *quadratic* models provide flexible representations of yields and macroeconomic variables through elegant pricing formulas. However, they have difficulties reproducing a short-term interest rate bounded from below, or its ability to stay at the lower bound for long periods, which limit their utility for policymakers confronted to a long-lasting ELB (Andreasen and Meldrum 2018). On the other hand, while *shadow-rate* models tackle the ELB-consistency successfully, it is at the expense of tractability. Moreover, as noted by Kim and Singleton (2012), this class of models show limited flexibility in macroeconomic dynamics with, for instance, stochastic volatility, such that they behave as a fully Gaussian model away from the ELB. Yet, each of these ingredients is critical to paint an accurate empirical picture of monetary policy and macroeconomic interdependence during the ELB (Fernandez-Villaverde and Rubio-Ramírez 2007; Coibon and Gorodnichenko 2011).

In this paper, I address the tension between tractability, ELB-consistency, and flexibility by introducing a new macro-finance framework named QARG that captures

macroeconomic and treasury curves dynamics at the ELB. I exploit the model to investigate the potential change in inflation dynamics when the economy reaches the ELB, the pricing of inflation components, and the policy response in such a low-yield environment. In my model, inflation dynamics are driven by expectation and volatility shocks, both of which are priced by investors. As a result, these shocks are reflected in long-maturity bond yields, risk premia, and in the likelihood of a binding ELB, even when the monetary policy rate is persistently stuck at its lower bound. A particular feature of the QARG model is that it does not assume an exogenous regime shift when the ELB starts binding, but rather uses information available throughout the pre- and post-ELB samples jointly to identify pricing relationships. Being able to provide an explicit link between inflation factors and sovereign yields during the ELB salvages the informativeness of yields and extends the traditional macro-finance models *à la* Ang and Piazzesi (2003).

Despite featuring nonlinearities, the QARG is particularly easy to handle because it belongs to the *affine-quadratic* class. First, nominal and real yields at any maturity are obtained as closed-form linear-quadratic functions of state variables, including inflation components. All nominal yields are consistent with the ELB, and the short rate can be persistently stuck there. Second, inflation and yields' expectations and volatility forecasts are available in closed form. Third, probabilities to stay at the ELB or to lift off are explicitly driven by the state variables. The availability of the above moments opens the door for survey data to be included in the estimation. Fifth, impulse-response functions are non-linear and state-dependent, but computable easily, allowing for an easy comparison of pre- and post-ELB results. Last, all observables are at most linear-quadratic combinations of the states, which greatly simplifies estimation with the quadratic filter of Monfort et al. (2015) as opposed to particle filtering. The estimation is then performed with pricing targets of 1- to 10-year maturity nominal and real U.S. treasury yields observed monthly from 1990 to the end of 2019, along with inflation and yield forecast survey data.

The estimation provides three takeaways. First, treasury yield curves uncover the existence of adverse inflation outcomes during the ELB period. Inflation trend and volatility filtered from the model show persistently large undershooting and overshooting, respectively, compared to the pre-ELB period. Looking at the pricing of inflation components, I show that these outcomes translate into large premia that drives elevated real yields. As the inflation central tendency falls and inflation uncertainty increases, deflation fears arise at short-maturities with an inflation risk premia component reaching -150bps. The amplitude of these negative premia are in line with the conditional mean model of Feunou and Fontaine (2014), and similar to the survey-based estimates of Camba-Mendez and Werner (2017). To the best of my knowledge, only Imakubo and Nakajima (2015) estimate a shadow-rate model to extract inflation premia from U.S. data, and they find consistently positive premia at about 80bps, but they do not fit realized inflation leaving too much flexibility to their model for inflation components. While my estimates for deflation fears are smaller at longer maturities, I find that nominal term premia grow with maturity, from virtually zero at 1y to between 0bps and 200bps during the ELB period for the 10y bond, while the expectation components are small and slowly moving. This result is in line with Imakubo and Nakajima (2015). In contrast, nominal premia estimates from Breach, D'amico, and Orphanides (2020) are lower than ours, mostly because they do not impose the ELB-consistency, and the short-rate is expected to increase more quickly than in the QARG. As a result, the QARG attributes most of the post-ELB increase in yields to term premia due to the ELB attraction for expected rates, while a standard quadratic model in the spirit of Andreasen and Meldrum (2018) attributes it to a rapid increase in expectations.

Second, a non-linear impulse-response analysis reveals that a monetary policy shock produces more diverse effects during a binding ELB period compared to normal times. I find that when the ELB is not binding, effects of tightening monetary policy shocks are fairly homogeneous. Inflation expectations go slightly down, and short-run

inflation risk premia decrease in reaction, but the overall effects are moderate. In turn, short-term yields stay elevated persistently leading to an overall increase in nominal and real yield curves. From 2009 to 2015, when the ELB is binding, lifting off by a few basis points can lead back to the ELB since such a shock was highly improbable at the time. The effects on inflation expectations are reversed, inflation volatility goes up unambiguously, and lifting off produces a wider range of effects, especially on long-maturity yields and inflation risk premia. This wider range of effects is consistent with the findings of Debortoli, Gali, and Gambetti (2020), although they focus more on the average effects. The ELB therefore hides a large heterogeneity during the 6 years where it is binding.

Third, I provide evidence that the choice to "*embrace the ELB*" (Williams (2009)) and to delay the increase of short-term rates (i.e. the liftoff) was in line with investors perceptions. I am the first to present the risk premium associated with a synthetic digital bond, paying off only if the economy is still at the ELB at maturity.[1] I find that this asset is considered a hedge by investors after 2009, as its premium is slightly negative when the ELB becomes binding. A further decomposition provides evidence that the pricing of inflation trend and volatility shocks contribute to lower these premia significantly, especially before 2011 for the latter. This complements the findings of Breach et al. (2020), in showing that inflation uncertainty impacts risk premia in the economy beyond those contained in nominal and real bonds.

This paper gathers both a modeling and an empirical innovation relative to the existing literature. For the former, the new QARG term structure model introduced below combines tractability for pricing nominal and real Treasuries, for the joint dynamics of their yields with macroeconomic components, as well as the ability to enforce a sticky effective lower bound. The affine-quadratic property is preserved by combining the non-negative gamma-zero process of Monfort et al. (2017) to represent

1. Bauer and Rudebusch (2016) present the expected ELB duration and model path under both risk-neutral and physical measures, but they do not discuss the risk premium associated with the liftoff.

the ELB-consistent short rate, with a standard quadratic term structure framework, which is known for its empirical performance (see Ahn et al. (2002), Leippold and Wu (2007)).[2] The estimated model shows appealing empirical properties, with low pricing errors on both nominal and real term structures (6bps and 11bps on average, respectively) with only four factors, and generates a substantially higher probability to reach the lower bound compared to a standard QTSM. As such, it complements the important study of Andreasen and Meldrum (2018) by expanding the range of available ELB-consistent affine and quadratic models.

Other approaches have been considered to produce an ELB-consistent pricing framework. The shadow-rate approach enforces the ELB and constitutes an alternative to the present model, stepping outside the class of closed-form models (see e.g. Kim and Singleton (2012)).[3] These models usually pose a challenge at the estimation stage, since pricing has to be approximate and show limited flexibility.[4] Interestingly, very few shadow-rate models have tackled the estimation of inflation risk premia components. Carriero et al. (2018) provide estimates for the UK though they do not directly fit realized inflation, Schupp (2020) for the Euro-Area, and Imakubo and Nakajima (2015) for Japan and the US. Conversely, by staying in the affine-quadratic world, the QARG model can be estimated quickly even incorporating macroeconomic and yields forecasts, as well as proxies for liftoff probabilities, in the set of empirical targets. This strengthens the identification of the joint macroeconomic and financial dynamics at virtually no cost, a particularly important feature when yields show limited variability at the ELB.

2. Alternative ELB-consistent models include Filipovic et al. (2017) linear-rational term structure model, Feunou et al. (2022) nearly arbitrage-free framework and Renne (2014) discrete states model.

3. Examples include and are not limited to Lemke and Vladu (2016), or Andreasen and Meldrum (2015) for yield-only models, Bauer and Rudebusch (2016), or Wu and Xia (2016) for macro-finance models. Carriero et al. (2018) employ a shadow rate model on nominal and real term structures jointly. Branger et al. (2016) incorporate a shadow rate in a long-run-risk model with inflation dynamics.

4. Approximate estimation methods for SR models have been developed by Kim and Priebsch (2013), Priebsch (2013), Wu and Xia (2016) and Christensen and Rudebusch (2015). Computationally intensive algorithms are also provided by Andreasen and Meldrum (2011) and Pericoli and Taboga (2015).

Second, my paper contributes to a strand of empirical literature devoted to understanding the dynamics of inflation through the study of nominal and real treasuries. Numerous term structure models have been developed to extract inflation dynamics and inflation pricing from asset prices (see e.g. Barr and Campbell (1997), Evans (1998), or Anderson and Sleath (2001)). However, most papers either do not consider ELB-consistency (Haubrich et al. (2012) or Fleckenstein et al. (2017)), are focused on the estimation of the relative liquidity of real bonds (e.g. Grischenko and Huang (2013), Abrahams et al. (2016), or D'Amico et al. (2018)) or are focused on inflation dynamics pre-ELB binding period (see Ang et al. (2008) Adrian and Wu (2009), and Campbell et al. (2017)). In contrast, the empirical exercise in this paper focuses on the potential change of interdependence between inflation components and asset prices in and out of the ELB. As such, it builds on the insights of both Mertens and Williams (2021) and King (2019) that a non-linear model is needed to understand the shift implied by an economy stuck at the ELB.

Last, this paper has implications for the literature looking at the relevance of the effective lower bound for macroeconomic models (see Gali (2018) for a survey of New Keynesian models). My empirical results resonate with the debate between Aruoba et al. (2017) and Reichlin (2015), on whether the ELB created a shift to a deflation equilibrium driven by expectation shocks. I find that inflation dynamics are indeed modified at the ELB. Cochrane (2017) advocates that none of the stark predictions of standard macroeconomic models on inflation are validated during the ELB period, and proposes a new model based on fiscal theory. Debortoli et al. (2020) show the irrelevance of the ELB for macroeconomic impulse-responses through a time-varying VAR. In turn, papers looking at asset prices show that there is a significant link between inflation components and treasury curves (see e.g. Ehling et al. (2018)), a moderate but significant change in inflation densities when the ELB is binding (see Mertens and Williams (2021)), or a change of correlation of inflation with stock returns (Gourio and Ngo (2020)) during the ELB. My paper contributes to this debate

by extracting information about inflation dynamics from asset prices using a reduced-form model, hence not taking a stand on the structural assumptions underlying the above works.

The remainder of the paper is organized as follows. Section 2 presents the formulation and the properties of the term structure model. I present the identification strategy and estimation method in Section 3, along with the fitting properties of the model. Section 4 presents the empirical results. Section 5 concludes.

2 A model for inflation risks and interest rates

I introduce the joint QARG asset pricing model for nominal and real yields and observable macroeconomic factors. While I formulate it directly with inflation dynamics, a more general specification is presented in internet Appendix B.1. I specify the pricing factors physical dynamics and express the nominal pricing kernel such that all yields are closed-form functions of the factors. Importantly, the framework imposes a lower bound for the nominal term structure.

2.1 Inflation central tendency and stochastic volatility

I assume that the dynamics of a $K \times 1$ vector of risk factors X_t are given by the following vector autoregression:

$$X_{t+1} = \mu + \Phi X_t + v_{t+1}\,, \tag{1}$$

where $v_{t+1} \overset{i.i.d.}{\sim} \mathcal{N}(0, \Sigma)$. This state vector contains three sets of variables, such that $X_{t+1} = \left(\pi^*_{t+1},\, \sigma_{t+1},\, y'_{t+1}\right)'$ where both π^*_{t+1} and σ_{t+1} are univariate and y_t is a vector of yield-specific risk factors of size $K_y \times 1$.

Inflation is defined as the year-on-year log-change of the CPI-U index, denoted by CPI_{t+1}, such that $\pi_{t+1} = \log(\text{CPI}_{t+1}/\text{CPI}_{t-11})$. Inflation dynamics are driven by the

first two elements of X_{t+1}, and the inflation rate is given by:

$$\pi_{t+1} = \bar{\pi} + \pi_t^* + \sigma_{t+1}\varepsilon_{t+1}^{\pi}\,, \tag{2}$$

where $\varepsilon_{t+1}^{\pi} \overset{i.i.d.}{\sim} \mathcal{N}(0,1)$, and is uncorrelated with v_{t+1}.

Equation (2) features both a long-run inflation component π_t^* and a high-frequency component driven by the stochastic volatility process σ_{t+1}. Having a persistent component representing inflation trend has become the standard in the literature on inflation modeling (see e.g. Cogley et al. (2010)), and in the asset pricing literature such as in Haubrich et al. (2012), Bansal and Shaliastovich (2013), or Feunou and Fontaine (2014). In the latter set of papers, the trend process is represented by a single factor, but it can feature heteroskedastic shocks, either replacing or adding to the heteroskedasticity of the realized inflation shock. I leave aside the heteroskedasticity of the inflation trend for parsimony.

Through the VAR specification of Equation (1), π_{t+1}^* can be Granger-caused by its own past π_t^*, past volatility σ_t and past yield factors y_t. The inflation dynamics are thus very close to those employed by Fleckenstein et al. (2017). In their model, inflation has a trend driven by two unobservable and homoskedastic Gaussian factors and inflation shocks feature stochastic volatility driven by a single factor, a structure similar to that of Equation (2).[5] In a similar fashion, my inflation specification can be interpreted as a particular case of Breach et al. (2020), who authorize inflation drift and volatility to be a linear combination of four homoskedastic Gaussian factors. In my framework, Equation (2) directly equates the first and second factors to inflation drift and volatility respectively, which would restrict some of their parameters to be zero. Last, and in line with Breach et al. (2020), my inflation shock ε_{t+1}^{π} is orthogonal to other shocks and unspanned by the nominal yield curve as it neither causes in the

5. An alternative specification for σ_{t+1} could be an independent Gamma process as in Fleckenstein et al. (2017). This would ensure positivity of the process but would lose the potential feedback effects with the other elements of X_t to preserve the closed-form pricing expressions in this context. The empirical impact of such a choice is left for future research.

state vector X_t, nor will it appear in the nominal short-term interest rate dynamics (see next section). This will allow my model to produce volatile short-lived inflation shocks.

2.2 An ELB-consistent short-rate specification with macroeconomic factors: QARG dynamics

In this economy, there exists a riskless n-maturity nominal investment accessible to investors at time t at price $P_t^{(n)}$. The one-month riskless yield is known at t and given by $r_t = -\log P_t^{(1)}$. Assuming no-arbitrage, r_t cannot in principle become negative since investors would just hoard cash otherwise, thus is bounded by the zero lower bound. In practice, there is an effective lower bound $\underline{r}$ that can differ from zero and the observed yield evolves above this ELB.

To reproduce this feature, I assume that the short-term yield is given by:

$$r_t = \underline{r} + z_t \,, \tag{3}$$

where z_t is a univariate non-negative process whose dynamics are given by a modified version of the autoregressive gamma-zero introduced by Monfort et al. (2017). These dynamics are defined through a mixing Poisson variable P_t, such that:

$$\mathsf{P}_t \,\big|\, (X_t,\, z_{t-1}) \sim \mathcal{P}\left(\alpha + \phi z_{t-1} + \kappa\beta' X_t + (\beta' X_t)^2\right) \quad \text{and} \quad z_t \,\big|\, \mathsf{P}_t \sim \Gamma\left(\mathsf{P}_t\,;\, c\right) \,, \tag{4}$$

where ϕ, κ, c and α are positive scalars, β is of dimension $K \times 1$, and P_t is the degree of freedom of the gamma distribution.[6] We denote these dynamics by $z_t | X_t, z_{t-1} \sim$

6. A sufficient condition for the intensity being positive is that $\alpha \geqslant \frac{\kappa^2}{4}$ and I impose that the equality holds for parsimony. Indeed, starting from a non-negative z_{t-1}, it is sufficient that $\alpha + \kappa\beta' X_t + (\beta' X_t)^2$ is non-negative to have a non-negative intensity. Such a condition is reached if the minimum of the quadratic function is non-negative. Having $x_{\beta,t} = \beta' X_t$, the minimum of $\alpha + \kappa x_{\beta,t} + x_{\beta,t}^2$ is reached for $x_{\beta,t} = -\frac{\kappa}{2}$, and the quadratic function yields $\alpha - \frac{\kappa^2}{2} + \frac{\kappa^2}{4} \geqslant 0 \iff \alpha \geqslant \frac{\kappa^2}{4}$.

$\text{QARG}_0\left(\alpha + \phi z_{t-1} + \kappa\beta' X_t + (\beta' X_t)^2 \; ; \; c\right)$, for quadratic autoregressive gamma-zer . In particular, we show in Appendix A.1 that z_t can be written:

$$z_t = c\left(\alpha + \phi z_{t-1} + \kappa\beta' X_t + (\beta' X_t)^2\right) + \varepsilon_t^z\,, \tag{5}$$

where ε_t^z is a martingale difference sequence conditionally on X_t and the past.

I obtain several implications from this specification. First, z_t is equal to zero as long as the Poisson draws P_t are equal to zero. This allows the short-rate process r_t to reach its lower bound $\underline{r}$ and potentially spend long periods there. Second, even though I allow only one linear combination of the state vector to enter the Poisson intensity for parsimony, the specification is general enough such that inflation mean and volatility factors π_t^* and σ_t as well as yield-specific factors y_t all impact the current one-period yield. As noted by Andreasen and Meldrum (2018) in the context of a standard quadratic model, this specification is supported by data and is barely restrictive. Last, the probabilities of reaching or getting away from the lower bound crucially depend on the current values of both inflation and yield-specific risk factors, namely X_t. The remaining properties of the gamma-zero distribution are detailed in Appendix A.1.

2.3 Short-rate dynamics: discussion

The QARG specification shares some features with quadratic term structure models (QTSM, see e.g. Ahn et al. (2002) or Breach et al. (2020)) However, Equation (4) defines a short-rate able to stay at the ELB, contrary to QTSMs. One key distinction of the model with respect to a standard QTSM is that it directly enables to identify periods when the lower bound $\underline{r}$ is binding, i.e. when realizations of z_t are equal to zero.

Additionally, the QARG allows for the time-varying Taylor rule feature of Ang et al. (2011), with monetary policy shifts. To gain some insight, Let us consider a

simple case where X_t consists only of the inflation trend π_t^* with zero mean, and where the ELB is zero. We can write:

$$r_t = \overline{r} + \underbrace{\rho \cdot r_{t-1}}_{\text{smoothing}} + (1-\rho) \underbrace{\left[1 + \frac{\beta}{\kappa}\pi_t^*\right] \frac{c\kappa\beta}{1-\rho}}_{\text{policy shift}} \pi_t^* + \varepsilon_t^z \,, \tag{6}$$

We can interpret the coefficients of the model in light of Equation (6). The coefficient $\frac{c\kappa\beta}{1-\rho}$ constitutes the baseline reaction of monetary policy to inflation expectation movements when inflation expectations are on target ($\pi_t^* = 0$). When the expectations deviate from target, monetary policymakers adjust their reaction function depending on how far the economy is from the steady state. It is easy to calculate the immediate response of the short-rate to a positive inflation trend shock $v_{1,t} = s$, given by $\beta^2 s^2 + [\kappa\beta + 2\beta^2 \mathbb{E}_{t-1}(\pi_t^*)] \times s$. We can directly see that the policy reaction is positively correlated with inflation expectations, a feature validated by data (see Figure 3 of Ang et al. (2011)), and consistent with the asymmetric policy response proposed by Bianchi et al. (2021). Notice that the general framework can readily include any measure of real activity in addition to inflation series to obtain a more standard Taylor rule specification.

2.4 The pricing kernel

I assume that the pricing kernel of the representative investor M_{t+1} is given by an exponential-affine function of the shocks to the risk factors:

$$M_{t+1} = \exp\left(- r_t + \lambda_t' \, v_{t+1} + \lambda_r \, [r_{t+1} - \mathbb{E}_t(r_{t+1})] - \xi_t \right) \tag{7}$$

where $\mathbb{E}_t(\bullet)$ is the conditional expectation operator given the filtration spanned by the history of $\{X_t, \pi_t, z_t\}$, and ξ_t is the convexity adjustment such that $\mathbb{E}_t\left(M_{t+1}\right) = e^{-r_t}$ (see internet Appendix B.2, and Appendix A.3 for their respective formulas). As in

Duffee (2002), the prices of risk are given by:

$$\lambda_t = \lambda_0 + \lambda_1 X_t \,. \tag{8}$$

Equation (7) features a time-varying price of risk for all the state variables shocks v_{t+1}, thus including inflation trend and volatility. As usual with this type of kernel, investors attribute a price λ_t to shocks v_{t+1}, and empirical estimates usually reflect that they fear positive inflation shocks. However, a second channel is at play when investors price unexpected shocks to the short rate. The latter is driven by squares of the Gaussian shocks v_{t+1}, and investors also price large deviations to their inflation components forecasts, whatever their sign. Such a channel is consistent with two-sided fears of inflation as documented for instance in Kitsul and Wright (2013).[7]

Despite the non-linearities in the pricing kernel specification, I show in Appendix A.4 that it has a self-preserving structure hence the risk-neutral dynamics of the risk factors are given by:

$$X_{t+1} = \mu^{\mathbb{Q}} + \Phi^{\mathbb{Q}} X_t + v_{t+1}^{\mathbb{Q}} \,, \tag{9}$$

where $v_{t+1}^{\mathbb{Q}} \overset{i.i.d.}{\sim} \mathcal{N}\left(0, \Sigma^{\mathbb{Q}}\right)$ and:

$$\begin{aligned}
\mu^{\mathbb{Q}} &= \left(I_K - 2\frac{\lambda_r c}{1-\lambda_r c}\Sigma\beta\beta'\right)^{-1}\left(\mu + \Sigma\lambda_0 + \frac{\kappa\lambda_r c}{1-\lambda_r c}\Sigma\beta\right) \\
\Phi^{\mathbb{Q}} &= \left(I_K - 2\frac{\lambda_r c}{1-\lambda_r c}\Sigma\beta\beta'\right)^{-1}\left(\Phi + \Sigma\lambda_1\right) \\
\Sigma^{\mathbb{Q}} &= \left(I_K - 2\frac{\lambda_r c}{1-\lambda_r c}\Sigma\beta\beta'\right)^{-1}\Sigma \,.
\end{aligned} \tag{10}$$

The risk-neutral dynamics of the short-rate factor z_t is then given by:

$$z_t \,\big|\, X_t,\, z_{t-1} \overset{\mathbb{Q}}{\sim} \text{QARG}_0\left(\alpha^{\mathbb{Q}} + \phi^{\mathbb{Q}} z_{t-1} + \kappa^{\mathbb{Q}}\beta^{\mathbb{Q}\prime} X_t + \left(\beta^{\mathbb{Q}\prime} X_t\right)^2 ;\, c^{\mathbb{Q}}\right) , \tag{11}$$

7. Note that it is possible to impose that inflation risks are unspanned by the nominal yield curve through linear constraints on the prices of risk and on the parameters driving the joint dynamics of yield-specific and inflation factors (see Joslin et al. (2014))

where $\alpha^{\mathbb{Q}}$, $\phi^{\mathbb{Q}}$ and $c^{\mathbb{Q}}$ are equal to their physical counterparts divided by $(1-\lambda_r c)$, and both $\kappa^{\mathbb{Q}}$ and $\beta^{\mathbb{Q}}$ are equal to their physical counterparts divided by $\sqrt{1-\lambda_r c}$.

2.5 Pricing the term structures

By no-arbitrage, the prices of nominal bonds of any maturity n are given by:

$$P_t^{(n)} = \mathbb{E}_t^{\mathbb{Q}}\left[\exp\left(-\sum_{i=0}^{n-1} r_{t+i}\right)\right], \tag{12}$$

where $\mathbb{E}_t^{\mathbb{Q}}(\bullet)$ is the risk-neutral conditional expectation operator given the filtration spanned by the history of $\{X_t, \pi_t, r_t\}$. In contrast, inflation-protected securities are securities paying off at maturity the realized inflation from issuance to maturity. For any maturity n, their prices are given by:[8]

$$P_t^{(n)^*} = \mathbb{E}_t^{\mathbb{Q}}\left[\exp\left(-\sum_{i=0}^{n-1} r_{t+i}\right)\frac{\text{CPI}_{t+n}}{\text{CPI}_t}\right], \tag{13}$$

Despite the non-Gaussian structure of the framework, I show in Appendix A.4 that the risk-neutral dynamics of inflation, of the risk factors and of the short-rate obtained in the previous Section define an affine-quadratic term structure model (QTSM) where the pricing Equations (12) and (13) can be obtained through closed-form recursions:

$$\begin{aligned} P_t^{(n)} &= \exp\left(\mathcal{A}_n + \mathcal{B}_n' X_t + X_t' \mathcal{C}_n X_t + \mathcal{D}_n z_t\right), \\ P_t^{(n)^*} &= \exp\left(\mathcal{A}_n^* + \mathcal{B}_n^{*\prime} X_t + X_t' \mathcal{C}_n^* X_t + \mathcal{D}_n^* z_t\right). \end{aligned} \tag{14}$$

The explicit recursions are functions of the risk-neutral parameters and are detailed in Appendix A.6. Corresponding continuously-compounded nominal and real yields are given by $R_t^{(n)} := -\frac{1}{n}\log P_t^{(n)}$ and $R_t^{(n)^*} := -\frac{1}{n}\log P_t^{(n)^*}$, respectively, and are

8. I discuss the specifics of real bonds in the Section detailing the data, notably the treatment of the so-called inflation lag used to compute their actual payoff.

linear-quadratic combinations of the risk factors.

The fact that the model belongs to the class of *affine-quadratic* models allows for several extremely useful features. Contrary to the shadow-rate model, I do not need to rely on any approximation or simulation technique to obtain the term structures since the pricing formulas are analytic (see for instance Wu and Xia (2016) or Christensen and Rudebusch (2015)). Second, the combination of physical and risk-neutral dynamics imply that forecasts of yields of all maturities at all horizons are obtained as closed-form linear-quadratic combinations of the risk factors. In particular, I show in internet Appendix B.2 that we can form a stacked risk factor $f_t = (X_t', X_t' \otimes X_t', z_t)$ that follows semi-strong VAR dynamics, such that:

$$f_t = \Psi_0 + \Psi f_{t-1} + \text{Vec}^{-1/2}\left(\Omega_0 + \Omega f_{t-1}\right)\zeta_t\,, \tag{15}$$

where ζ_t is a martingale difference with zero mean and unit variance. The conditional moments are easily obtained rolling over the VAR formulation.

Although the previous properties are usually available in a standard QTSM, the gamma-zero distribution properties provide the conditional probabilities to stay at the ELB for any length n as a closed-form function of the factors:

$$\mathbb{P}_t\left(r_{t+1:t+n} = \underline{r}\right) = \exp\left(\mathcal{A}_n^{\mathbb{P},(\text{elb})} + \mathcal{B}_n^{\mathbb{P},(\text{elb})'} X_t + X_t' \mathcal{C}_n^{\mathbb{P},(\text{elb})} X_t + \mathcal{D}_n^{\mathbb{P},(\text{elb})} z_t\right)\,, \tag{16}$$

where the loadings are given through closed-form recursions in Appendix A.7. These two points prove particularly useful in practice for improving the quality of the estimation through the use of forecast data, both for yields levels and liftoff probabilities (see e.g. Kim and Orphanides (2012)). I include both in the empirical application below.

3 Estimation Strategy

3.1 Identification strategy and data

I consider monthly U.S. data from January 1990 to December 2019, to avoid any issue related to the Covid19 period. Since the focus is on the ELB period, the four years of moderate increase (2015-2019) provide useful information about the liftoff. I obtain the 3-months nominal interest rate from the H.15 data on the Federal Reserve website and longer nominal zero-coupon yields for maturities of 1, 2, 3, 5, 7, and 10 years from Gurkaynak et al. (2007). For real bonds, I compute synthetic yields by subtracting zero-coupon inflation swap rates of maturities of 1, 2, 3, 5, 7, and 10 years obtained from Bloomberg to the corresponding-maturity nominal bond (as e.g. Christensen and Gillan (2012) or Moench and Vladu (2018)).[9] The inflation-linked swap data start in July 2004. I treat the months following Lehman failure – from September 2008 to February 2009 – as missing data since most movements on the inflation-linked securities interest rates during this period can likely be attributed to the disruption of the inflation-indexed market (see for instance D'Amico et al. (2018)). The year-on-year inflation rate is computed from the CPI-U series of the BLS database, and is lagged of 3 months to be consistent with the reference price index used for inflation-indexed payments.

To better identify the joint dynamics of yields and inflation, I follow Kim and Orphanides (2012) and Chernov and Mueller (2012) adding two sets of survey forecasts in the observable variables. I obtain series of expected average inflation over the next 1 and 10 years and nominal yields forecasts for the 10-year maturity, 3-months and

9. Christensen and Gillan (2012) note that though not free from liquidity risk, inflation swaps are less likely to be affected by liquidity issues compared to TIPS. For papers who focus on extracting the liquidity risk from TIPS data, see for instance Sack and Elasser (2004), Shen (2006), Gurkaynak et al. (2010), Grischenko and Huang (2013), Pflueger and Viceira (2016) or D'Amico et al. (2018). Fleckenstein et al. (2014) note that the TIPS bonds were also subject to large mispricing during the crisis, which can be explained partly by sovereign default risk (Dittmar et al. 2022), especially after 2010.

Figure 1: Nominal and real term structures and inflation data

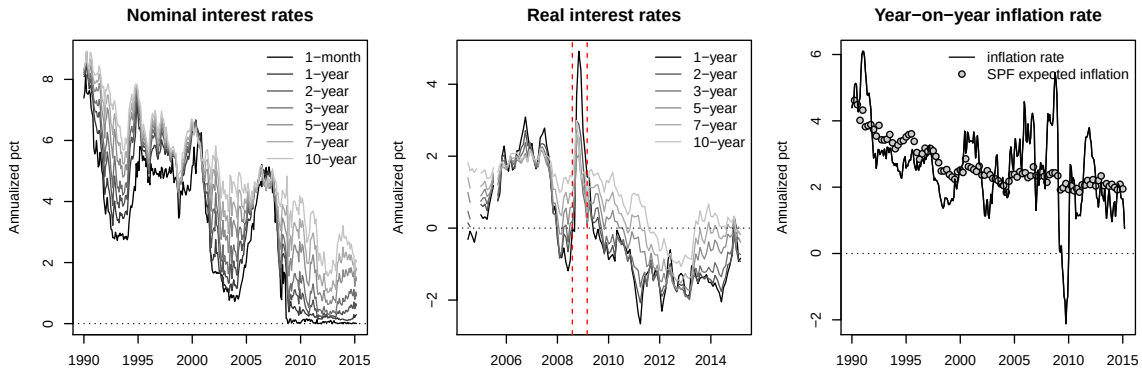

Notes: The left plot presents the time-series of the nominal term structure of interest rates from January 1990 to December 2019. Maturities range from 3 months to 10 years. The middle plot presents the term structure of real rates built as the difference between the nominal zero-coupon interest rates and the inflation swap rates of the same maturity. Observations start in July 2004 and run to December 2019. The vertical red dashed lines indicate the beginning and end of a reduced market liquidity period, that we treat as missing data in the estimation. The right plot presents the realized year-on-year inflation lagged of 3 months (black solid line). The dots superimpose the expected average inflation rate over the next year as measured by the survey of professional forecasters.

Table 1: Descriptive statistics

	Nominal rates (1990-2019)						
	3-month	1-year	2-year	3-year	5-year	7-year	10-year
mean	2.771	3.062	3.308	3.542	3.954	4.290	4.661
sd	2.280	2.322	2.307	2.250	2.126	2.033	1.948
$\rho(1)$	0.988	0.989	0.987	0.986	0.985	0.984	0.984
	Inflation	(Synthetic) Real rates (2004-2019)					
	y-o-y	1-year	2-year	3-year	5-year	7-year	10-year
mean	2.434	−0.108	−0.116	−0.037	0.210	0.461	0.744
mean (excl. crisis)		−0.211	−0.186	−0.088	0.170	0.419	0.701
sd	1.252	1.391	1.223	1.119	0.978	0.913	0.864
sd (excl. crisis)		1.255	1.167	1.091	0.965	0.893	0.840
$\rho(1)$	0.951	0.940	0.964	0.965	0.968	0.962	0.960

Notes: All units are annualized percentage points. 'mean' are sample averages, 'sd' are sample standard deviations, and '$\rho(1)$' are autocorrelation of order 1. The 'excl. crisis' rows present descriptive statistics calculated on the synthetic TIPS data – the nominal yields minus the corresponding maturity inflation-linked swap rate – excluding the period from September 2008 to February 2009.

1-year ahead from the Philadelphia Fed surveys of professional forecasters database. All these surveys are quarterly, and are computed as the mean forecast across respondents. To guide longer-term forecasts, I add the 10-year forecast of the 3-month TBill rate from the same survey data, available at the yearly frequency. For all these survey

data, I gather the mean forecast produced by respondents. Last, I extract data about the probabilities of seeing no interest rate increase by the Fed between each date and one year ahead from the primary dealer survey conducted by the New York Fed. I collect information starting from January 2011. Details on these computations are provided in internet Appendix B.4. Time series and standard descriptive statistics of interest rates and inflation are presented in Figure 1 and in Table 1. Surveys and ELB probability series are represented in Figure 2.

3.2 The state-space formulation

All observables except two are closed-form linear-quadratic combinations of the state variables X_t and z_t. On the one hand, the probabilities to stay at the ELB are exponential linear-quadratic functions of the states (see Equation (16)). I therefore take the natural logarithm of the probabilities data. On the other hand, inflation dynamics involve the i.i.d. shocks ε_t^π and the lag of π_t^* which are not readily included in our state variables VAR. I take care of this issue augmenting the states as $X_t^{(aug)} = (X_t', \varepsilon_t^\pi, \pi_{t-1}^*)'$ without changing their VAR structure.

$$X_t^{(aug)} = \begin{pmatrix} X_t \\ \varepsilon_t^\pi \\ \pi_{t-1}^* \end{pmatrix} = \begin{pmatrix} \mu \\ 0 \\ 0 \end{pmatrix} + \begin{pmatrix} \Phi & 0 & 0 \\ 0 & 0 & 0 \\ e_1' & 0 & 0 \end{pmatrix} \begin{pmatrix} X_{t-1} \\ \varepsilon_{t-1}^\pi \\ \pi_{t-2}^* \end{pmatrix} + \begin{pmatrix} I & 0 \\ 0 & 1 \\ 0 & 0 \end{pmatrix} \begin{pmatrix} v_t \\ \varepsilon_t^\pi \end{pmatrix}, \tag{17}$$

where e_1 the first column of the identity matrix, such that $e_1' X_{t-1} = \pi_{t-1}^*$.

I now turn to the state-space formulation of the model. To fix ideas, consider that all our observables at time t are gathered in a vector denoted by $\mathcal{Y}_t^{(obs)}$. This vector contains all 13 yields, the inflation rate, 5 inflation and yields survey series and one ELB log-probabilities series. I assume that all these observables except inflation are

measured with errors, and write:

$$\mathcal{Y}_t^{(obs)} = \mathcal{A} + \mathcal{B}' X_t^{(aug)} + \mathcal{C}\,\text{Vec}\left(X_t^{(aug)} X_t^{(aug)'}\right) + \mathcal{D}\, z_t + \eta_t\,, \tag{18}$$

where each element of η_t is independent and $\eta_{i,t} \overset{i.i.d.}{\sim} \mathcal{N}(0, \omega_i^2)$ are the measurement errors. For parsimony, I assume the the standard deviation of the measurement errors is the same across nominal yields on the one hand, across real yields on the other hand. Additionally, to take care of potential liquidity issues remaining in real yields, I impose that the standard deviations of their measurement errors each month is proportional to hte liquidity index of Abrahams et al. (2016).[10] For survey data, ω_i is calibrated to the average forecaster disagreement.

I consider 2 latent yield-specific factors y_t ($K_y = 2$). Without further assumptions, the latent factors can still be rotated and are not uniquely identified. I therefore impose several constraints on the parameters driving the dynamics of our risk factors. The conditional covariance matrix Σ is diagonal and the part corresponding to y_t is set to identity. I impose that the autoregressive matrix Φ is full for π_t^* and σ_t and upper-triangular otherwise, so all factors can feedback on π_t^*.[11] For identification, I also impose that the model-implied mean of π_t^* is null so that average inflation is given directly by $\bar{\pi}$.

Since the measurement equations (18) are linear-quadratic in the states and all states form an affine process, I can readily estimate the QARG model using the *Quadratic Kalman filter* of Monfort et al. (2015). The method allows to take care of the quadratic part of the state-space model more efficiently than standard approxi-

10. I thank Richard Crump for providing the data, which is presented on Figure IA.4 of the internet Appendix.

11. Joslin et al. (2011) use a different identification scheme where the variance-covariance can be full, the $\mathbb{Q}$ autoregressive matrix is in real jordan form, and the short-term interest rate has a unit loading on all latent factors. Their canonical representation and the one used in this paper are equivalent, and both have the same number of identification restrictions. In addition, I prefer estimating β and fixing the conditional variance of the factors rather than the other way round to authorize some factors to potentially be nearly unspanned without shrinking their conditional volatility.

mate non-linear filters such as the extended and unscented Kalman filters, although the latter methods could be used as well. The algorithm is detailed in internet Appendix B.3.[12]. Last, I add a penalty to the likelihood forcing the model to reproduce the mean of the 3-month and 10-year nominal yields.

3.3 Fitting properties

For the sake of space the estimated parameters can be found on Tables A.1 and A.2 in the Appendix. The model is able to provide both a reasonable fit on the SPF data that is tracking down closely the observed series (see Figure 2), and an impressive fit on both term structures with only 4 factors. RMSEs range from 3.5bps to 8bps for nominal rates and from 8bps to 17bps for real rates (see Table 2). These fitting properties are comparable to the model of Abrahams et al. (2016), who use a 5-factor ATSM to fit both yield curves. In comparison, my model only has 4 factors, two of which are identified by inflation dynamics. Quadratic models are well-known to fit yields more efficiently than a pure linear model with the same number of factors (see e.g. Leippold and Wu (2007)).

I check that both objective and risk-neutral dynamics are well-identified by performing the LPY tests of Dai and Singleton (2002)[13]. Models relying on positive processes usually have difficulties passing these tests (see e.g. Backus et al. (2001)). Conversely, Figure IA.1 and Table IA.2 of the internet Appendix show that both conditions cannot be rejected at the 5% level, thus validating the empirical estimates.

12. Alternatively, the sequential regression approach of Andreasen and Christensen (2015) could be used for estimation since the model is of the affine-quadratic class. In any case, these methods allows for one likelihood call in less that 1 second on a standard computer, facilitating numerical issues compared to particle filtering, the standard method for evaluating complex likelihoods (see e.g. Fernandez-Villaverde and Rubio-Ramírez (2007))

13. see internet appendix B.5 for details about these tests in the present setting.

Figure 2: Fitted series of survey data

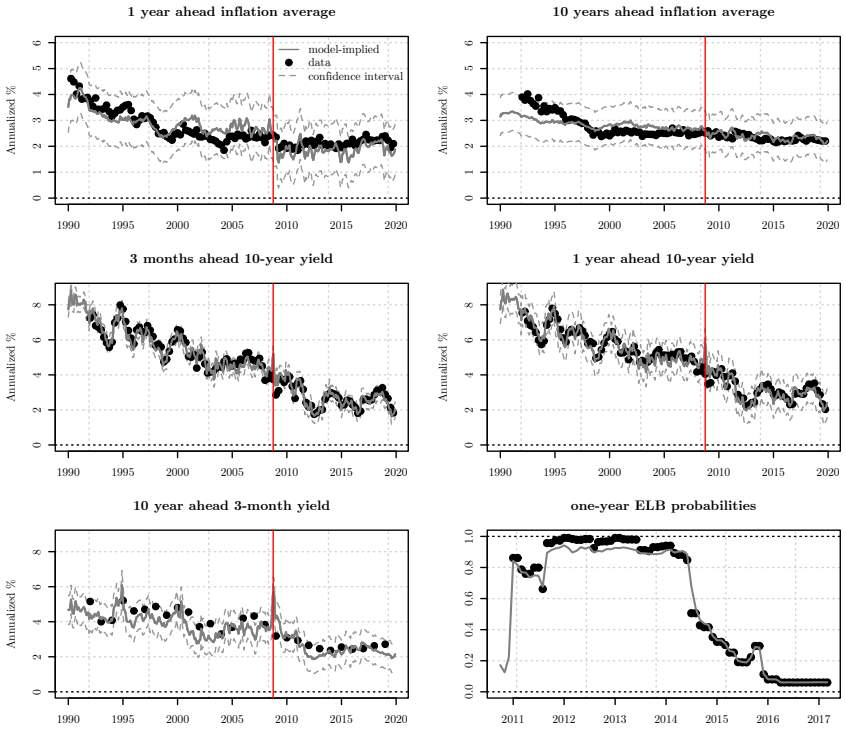

Notes: The black dots correspond to observed forecast data. The grey solid lines correspond to the model-implied forecasted values. Top graphs correspond respectively to the one-year ahead and 10-year ahead inflation average surveys. Medium graphs correspond respectively to the three-months ahead and one-year ahead 10-year yield survey. Units are in annualized percentage points. Bottom graphs correspond respectively to the 10y forecast of the 3m TBill and the fitted one-year ELB probabilities. Confidence intervals computed using the measurement errors standard deviations are plotted in grey dashed lines. The red vertical line delimits the beginning of the effective lower bound period.

4 Empirical Results

4.1 Inflation dynamics at the lower bound

An important question that has arisen in the macroeconomic debate is whether reaching the ELB fundamentally changes inflation dynamics. The estimated model provides a natural answer to that question by using both inflation data and a cross-section of treasury yields to back out inflation trend and volatility time series. The filtered factors are presented on Figure 3, along with the date at which the the ELB starts binding.

The estimated inflation central tendency and volatility both exhibit a large shift

Table 2: Model fit and characteristics

	Panel (a): QARG model						
Maturities (months)	1	12	24	36	60	84	120
Nominal rates RMSE (bps)	7.51	7.78	7.06	5.29	4.02	3.49	5.09
Real rates RMSE (bps)	-	17.07	8.68	7.75	9.97	11.64	12.32
Probabilities (in %)	$\mathbb{P}(r_t = \underline{r}) = 33.89$			$\mathbb{P}(r_t = \underline{r} \vert r_{t-1} = \underline{r}) = 71.86$			
	$\mathbb{P}(r_t < 25bps) = 36.98$			$\mathbb{P}(r_t < 25bps \vert r_{t-1} < 25bps) = 72.97$			

	Panel (b): Standard QTSM						
Maturities (months)	1	12	24	36	60	84	120
Nominal rates RMSE (bps)	6.64	8.11	7.45	8.36	7.63	6.25	6.00
Real rates RMSE (bps)	-	15.80	5.83	7.25	8.81	10.00	9.98
Probabilities (in %)	$\mathbb{P}(r_t < 25bps) = 9.72$			$\mathbb{P}(r_t < 25bps \vert r_{t-1} < 25bps) = 83.13$			

Note: Probabilities are calculated with simulated paths of length 100,000.

Figure 3: Filtered factors

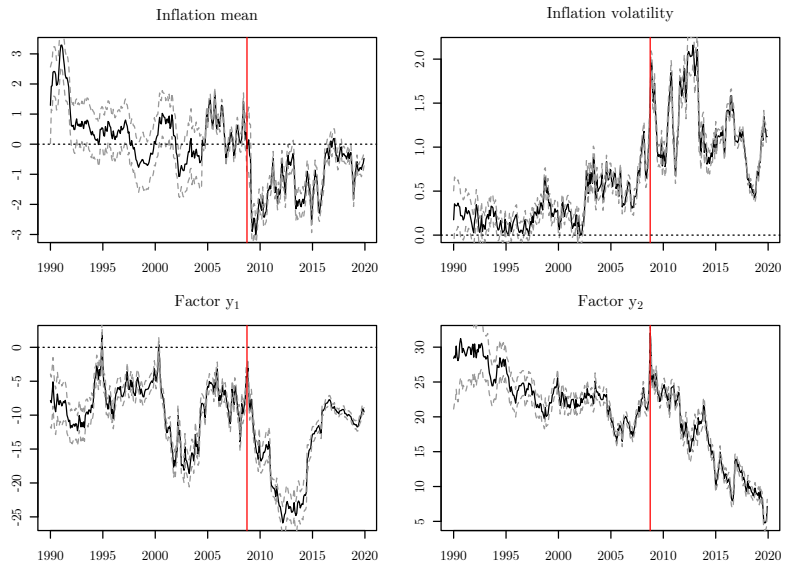

Notes: The unit for inflation central tendency π_t^* and inflation volatility σ_t is in percentage points. Grey dashed lines are 95% confidence bands. The red vertical line delimits the beginning of the effective lower bound period.

at the ELB, pointing towards a change in inflation dynamics. The inflation trend π_t^* mostly fluctuates around zero between 1990 and 2009, jumps to $\pi_t^* = -3\%$ in 2009, leading to an inflation forecast of $\overline{\pi} + \pi_t^* = -0.57\%$. It stays consistently in the negative territory afterwards. A similar phenomenon can be seen for inflation

volatility, which is comprised below 1% before the ELB starts binding, but spikes up to 2% and stays elevated during the whole ELB period.

The identification of inflation components through bond yields reveals that the ELB episode in the U.S. resulted in persistent adverse inflation shocks, where inflation stayed below target with a large volatility during the five ELB-binding years. This empirical evidence supports the view that the ELB resulted in a prolonged low inflation/deflation regime at the ELB (Aruoba et al. 2017). These stylized facts are hard to identify using historical inflation data only as in e.g. Debortoli et al. (2020), but can be unveiled by the use of asset prices.

4.2 Interest rates at the ELB

While the short-term nominal rate is stuck at the ELB, long-term rates continue to move. The prolonged low inflation trend observed at the ELB pushes real yields upward, slowing down the recovery. Swanson and Williams (2014) argue that these long-term rates have been virtually unaffected by the ELB, possibly because of nominal and inflation term premia responsiveness to news occurring during the period. Whether yields are dominated by risk premia rather than expectations is an empirical question.

I provide the historical decomposition of expectation and risk premia components observed during the ELB period on Figure 4. The 1-year and 10-year expectation components become virtually null and below 200bps, respectively. The latter is slowly moving, as indicated by survey data, emphasizing the stability of investors expectations that short-term interest rates will remain low for a long period of time. This leads most of the nominal yields fluctuations to be explained by the term premium that investors require to hold these bonds. During the ELB period, the 1-year nominal risk premia component is null whereas most of the 10-year nominal term premium is consistently positive and volatile, fluctuating between 0bps and 200bps. Most of the responsiveness of the long-run nominal yields during the ELB can therefore be

attributed to fluctuations in the term premium.

Figure 4: Decomposition of interest rates

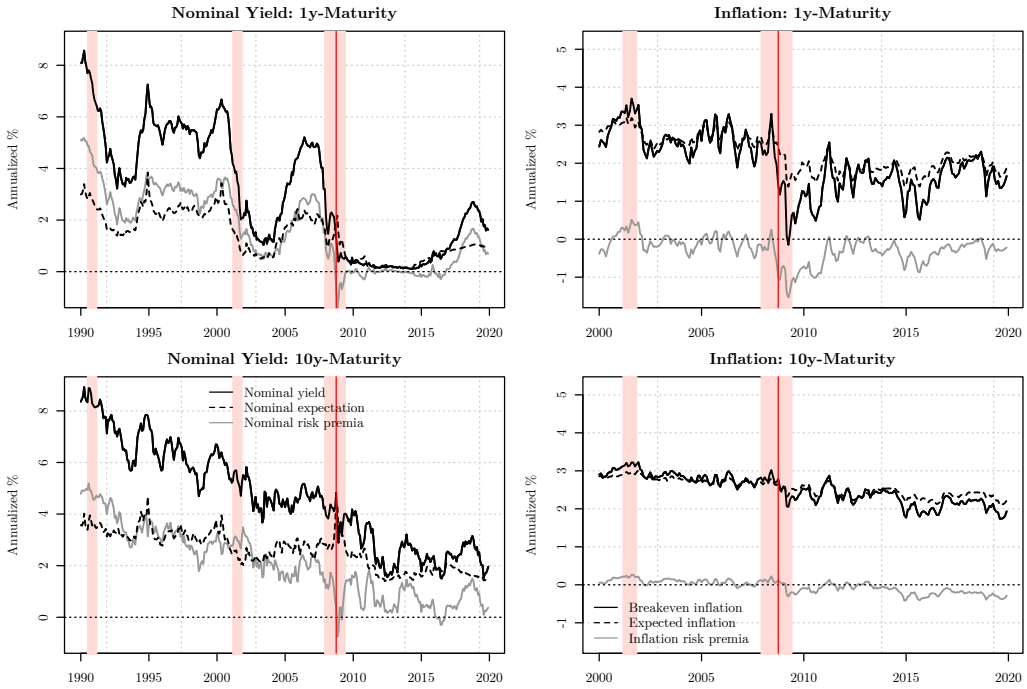

Notes: The first column presents results for the nominal yields components, whereas the second column presents results for the inflation components. The first row presents to the observed data (black solid line), the risk premia (grey solid line), and the expected component (black dashed line) at the one year maturity. The second row presents the same components at the 10 year maturity. Units are in annualized percentage points. The red vertical line delimits the beginning of the effective lower bound period. Pink shaded areas are NBER recession periods.

On the inflation risk premia series (IRP, right panel of Figure 4), the empirical estimates show inverted patterns with respect to maturity compared to nominal term premia. At the short-end, the ELB coincides with a surge in deflation fears with the IRP reaching an all time low of -150bps. The post-2009 period shows a convergence to close-to-zero historical values but the inflation risk premium stays consistently negative between 0 and -100bps. Conversely, the 10-year inflation premium component has a low volatility, and slowly fluctuates around 0. When the ELB hits, the long-run IRP goes to a moderate $-30bps$.

Translating these to real components by subtracting nominal and inflation components, the U.S. experienced heightened short-term yields not only because of a

drop in inflation expectations, but because of significant short-run deflation fears. At the ELB, the 1y TIPS yields would have reached -1.5% absent deflation fears compared to about 0% historically. At the long-end, the containment of deflation fears plays favorably for real yields. However, notably through increased inflation volatility, nominal uncertainty is significant and drives 10y real yields upwards.

4.3 Discussion of inflation risk premia estimates

Risk premia estimates are only as good as the term structure model. While I have confirmed previously that the fitting properties of my model were satisfactory, it is useful to compare the risk premium estimates to previous literature to gain some perspective. Fleckenstein et al. (2017) estimate a positive and stable 1-y inflation premium (IRP henceforth), contained between 0bps and 30bps on a 2009/2015 sample. In comparison, their 10-y inflation premium is very volatile, peaking at 80bps in January 2010 and going to negative territory at -35bps from early 2015 onwards. This is opposite to what I find here, but they do neither use survey data nor inflation data in the estimation.

Haubrich et al. (2012) impose risk premia estimates to be functions of the conditional volatility of interest rates only. This produces long-term real term premia and inflation risk premia that are consistently positive, contrary to my estimates. Short-term inflation premia estimates are mostly negative, and also show a large dip up to -80bps in 2009 similarly to my model. Their data stops in 2010 preventing the authors from drawing a conclusion on the ELB period as a whole.

Abrahams et al. (2016) produce obtain a 10-y IRP fluctuating between -40bps and 90bps from 2000 to 2014. Feunou and Fontaine (2014) also obtain a large dip of short-term inflation premia when the economy hits the ELB, and consistently negative estimates afterwards. Breach et al. (2020) find a 2y and 10y IRP negative during the ELB period (about -50bps) but more pronounced business cycle fluctuations. The IRP estimates provided by my model show a time-series behavior and magnitudes

consistent with these last two papers. The sign of my IRP estimates are particularly in line with the model-free estimates of Camba-Mendez and Werner (2017). However, the ELB constraint on nominal yields is unique to my framework and allows to uncover the particular pattern of a large dip detailed above, with a larger magnitude for the short-run IRP.

Last, a few papers extract inflation premia from ELB-consistent shadow rate models. Carriero, Mouabbi, and Vangelista (2018) findings on UK data imply that inflation expectations jump down persistently so inflation premia jump to more than 200bps when the economy hits the ELB. They however do not use survey data to discipline the term structure model. Schupp (2020) finds moderately negative IRP estimates on Euro-area data, similarly to this paper. The fact that my model is easy to estimate and to combine various survey data allows for a richer information set to identify IRP.

4.4 Comparison with a standard QTSM

To confirm the added value of the ELB-consistency to the quadratic structure of my framework, I estimate a standard QTSM without the gamma-zero variable but with the same structure as presented in Section 2, very close to the one in Andreasen and Meldrum (2018). I replace Equations (3) and (4) by: $r_t = \underline{r} + \kappa\beta' X_t + (\beta' X_t)^2$.

First, consistently with the findings of Andreasen and Meldrum (2018), both models produce virtually the same fit of the term structures (see Table 2). Second, I focus on the ELB for both models and compare the model-implied probabilities of obtaining interest rates below 25bps. Obtaining direct probabilities of being at the ELB is impossible for the standard QTSM, which treats the lower bound as a reflecting barrier and the short-term interest rate bounces back immediately after reaching it. The difference is striking: the QARG implies a 34% probability to reach the ELB and a 37% probability to obtain a short-term interest rate below 25bps while the standard QTSM-implied probability for staying below 25bps is only 10% (Table 2).

Interestingly, the probability to stay below 25bps for two consecutive periods is in the same ballpark and elevated. This can be explained by the fact that the standard QTSM estimates implies a persistent short-term yield irrespective of whether the ELB is binding. Figure 5 presents 2-year ahead mean forecasts of the two models to illustrate that feature. My model (QARG, in blue) usually implies a seemingly faster mean-reversion than the QTSM (in red), even during the ELB because it implies a larger short-rate volatility. The mode implied by the QARG is the lower bound. In turn, when interest rates are high, my model produces forecasts that decrease quite fastly but feature a reversal after a year, in line with potential business cycle fluctuations.

Figure 5: 2-year ahead forecast comparison for the 3-month yield

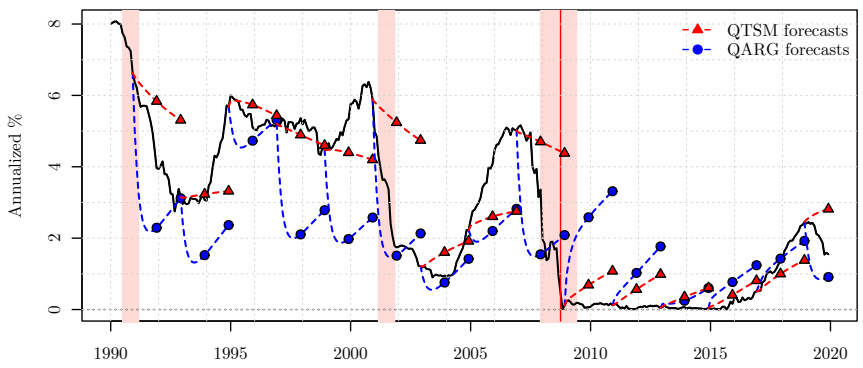

Notes: The black solid line presents the time series of the observed 3m yield. Blue dashed lines present the forecasts implied by the QARG while red dashed lines present the forecasts implied by the standard QTSM. These forecasts are presented from each point every two years for two years out. Each large dot of the corresponding color emphasizes the point forecast one and two years ahead.

Last, I compare the term premia decomposition implied by the two models on Figure 6. While inflation premia are roughly in line with each other between the two models, nominal premia differ widely. The high persistence of the QTSM implies that the expectation component at the 1-year maturity follows the observed yield quite closely. In contrast, my model produces a lower forecast of the short-term interest rate one-year ahead due to the ELB attraction. Thus, after the 2015 liftoff, my model implies that the short-term yield increases mostly because of risk premium, while the

QTSM implies that nearly all increase is expectation-driven. The differences are smaller on the 10-year yield decomposition (bottom-left panel of Figure 6). Indeed, both expectation series are driven by the survey forecaster data. However, yet again at the end of the sample the expectation component implied by the QTSM climbs up while the QARG explains the higher nominal yields mostly through a rise in the risk-premium. These results thus complement the analysis of Andreasen and Meldrum (2018), by showing that my model shares the same fitting properties as a standard QTSM but produces different term premia decomposition due to the presence of the ELB point mass.

Figure 6: Decomposition of interest rates: QARG v. QTSM

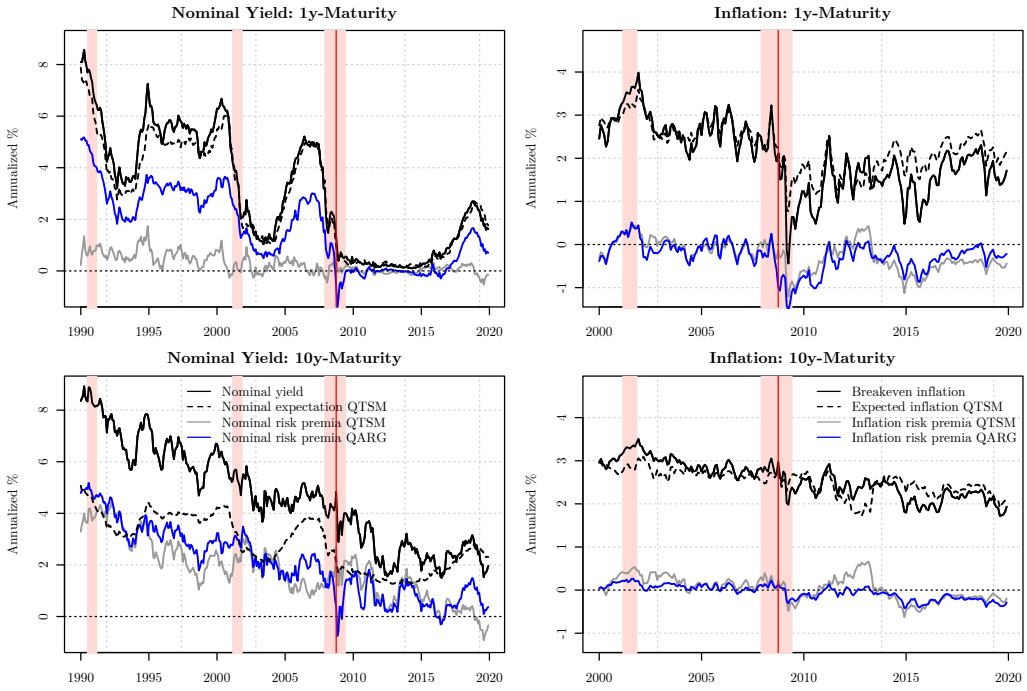

Notes: The first column presents results for the nominal yields components, whereas the second column presents results for the inflation components. The first row presents to the observed data (black solid line), the risk premia (grey solid line), and the expected component (black dashed line) at the one year maturity. The second row presents the same components at the 10 year maturity. Units are in annualized percentage points. The red vertical line delimits the beginning of the effective lower bound period. Pink shaded areas are NBER recession periods.

4.5 The effect of monetary policy shocks at the lower bound

A natural question to ask is whether monetary policy can help getting out of the deflation trap. In particular, Aruoba et al. (2017) suggest that lifting-off from the ELB may increase inflation expectations and allow the economy to escape the deflation state, mostly through the Fisher effect. While this counterintuitive effect is debated by Reichlin (2015), the effect of monetary policy shocks at the ELB lacks empirical evidence. I investigate policy responses below.

I derive impulse-response functions to observe the effect of a liftoff shock on inflation components and asset prices in the economy. Note that the model inherently embeds nonlinear dynamics through the short rate specification (4). Both magnitude and sign of impulse-responses thus critically depend on the starting state. This property is conform with the fact that the ELB represents a different regime and that the reaction of asset prices to the exact same shocks can be different in normal times and during the ELB (Lansing 2021, for instance). A key advantage of the framework is that impulse-responses for each of these variables of interest are obtained in closed-form.

I perform impulse-responses resulting from a tightening monetary policy shock starting from each date in the sample. To make sure that the liftoff shock is independent from inflation shocks, I impose that it is fully reflected by shocks to the yield-specific factors y_t.[14] The size of the shock is equal to the conditional volatility of the short-term interest rate at the starting date. These tightening/liftoff shocks range from 1bps to 8bps. I group the IRFs over two sub-periods and compare the effects: *(i)* ELB not binding, *(ii)* ELB-binding period [2009-2015]. I grouped the results accordingly and computed the median, min and max responses over these sub-periods. The entire methodology is detailed in Appendix A.8, and the results are presented on Figure 7.

14. The only requirement is that the shock is orthogonal to inflation trend and inflation volatility shocks. This shock cannot be interpreted as a *structural* monetary policy shock, as it could be caused by another variable outside of the model such as output gap for instance.

Figure 7: Impulse-response functions: liftoff shock

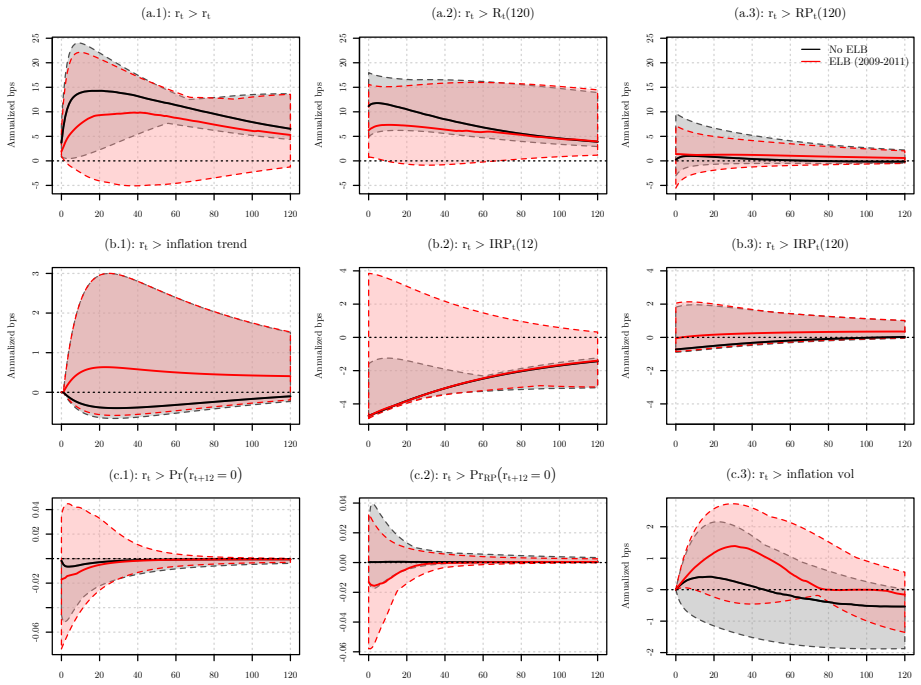

Notes: These graphs present the IRFs of an increase in the short-term nominal interest rate. Panel (a) presents the effect on the nominal side of the term structure, namely the short-term interest rate (a.1), the 10y yield (a.2) and the 10y risk premium (a.3). On panel (b), we find the effects on inflation components, namely inflation itself (b.1), 1y inflation risk premium (b.2) and 10y inflation risk premium (b.3). Panel (c) presents the effects on the 1y ELB probability (c.1), the 1y ELB risk premium (c.2) and the inflation volatility (c.3). Grey- and red-shaded areas represent the min-max range of possible outcomes given the different initial values respectively starting from a non-ELB or a ELB state. solid lines of the same color are the associated median responses. Units are in annualized basis points.

The IRFs show different features depending on the considered subsample. In normal times, a tightening monetary policy shock tends to be accompanied by further increases up to 15bps after a year, and slowly decays afterwards. This shock raises the term structure mostly through the expectation component so the yield curve flattens. Inflation expectations decrease by only 1bp, while both short and long-run inflation risk premia go down by 4bps and 1bp, respectively, and inflation volatility does not move much. These are fairly moderate effects, and shows that monetary policy had low impact on inflation components, in particular inflation volatility.

A binding ELB produces distinct effects. First, the effects have a wider uncertainty on most of the response variables. The size of the initial shock produces a maximum

of 10bps on the short-term interest rate. However, the short-term interest has a significant chance to go down after a couple of months such that the ELB becomes binding again. After 5 years, the initial shock turns into a [-5bps, 13bps] when the ELB is binding, compared to [7bps, 13bps] during normal times. This trickles down to the longer-run expectation component, and the 10-year yield response is lower than in normal times, at 7bps after a year. In comparison, the effect on term premia is virtually identical during the two periods. Since the distribution of effects on the short-rate comprises the negative range, probabilities to reach the ELB can increase by as much a 4pp and ELB risk premia can decrease by up to 6pp, emphasizing ELB desirability (see next section).

In sum, this analysis shows that during the ELB period, lifting off produces more diverse effects than during normal times and a greater potential to go back to a binding ELB. The ELB therefore hides a wide range of states that needs to be carefully assessed before lifting off.

4.6 Embracing the lower bound

Early on in the crisis, Williams (2009) called for an "embrace" of the lower bound by leaving short-term nominal rates to close to zero values for a substantial amount of time. One way to analyze efficiency of this policy from the investors' point of view is to measure whether staying at the ELB is associated with high or low marginal utility empirically, and look at the ELB event risk premium. For simplicity of exposition, consider that the effective lower bound parameter is null ($\underline{r} = 0$). Using the model estimates, I form the price of an ELB Arrow-Debreu security, providing \$1 if and only if the ELB binds between today and any date $t+n$ in the future. Such a price $P^{(n)}_{elb,t}$ is given by:

$$P^{(n)}_{elb,t} = \mathbb{E}^{\mathbb{Q}}_t \left[\exp\left(-\sum_{i=0}^{n-1} r_{t+i} \right) \times \mathbb{1}\left\{ r_{t+1:t+n} = 0 \right\} \right] = \mathbb{Q}_t \left[r_{t+1:t+n} = 0 \right] . \tag{19}$$

Equation (19) equates the price of the ELB Arrow-Debreu security with the risk-neutral probability to stay at the ELB. In the model, these probabilities are given by the risk-neutral counterpart of Equation (16). Similarly, the price of this bond purging from the risk premium is given by the physical probability to stay at the ELB, i.e. $\mathbb{P}_t\left(r_{t+1:t+n}=0\right)$. These physical probabilities are the one fitted by the model consistently with the primary dealer survey data. The ELB risk premium can be defined as:

$$\mathrm{RP}_{elb,t}^{(n)} = \frac{1}{n}\log\left(\frac{\mathbb{Q}_t(r_{t+1:t+n}=0)}{\mathbb{P}_t(r_{t+1:t+n}=0)}\right). \tag{20}$$

This risk premium is positive (negative) when staying at the ELB coincides with states of high (low) marginal utility. I thus interpret a falling risk premium as indicative of an increased desirability of a binding ELB in the future, or fear of lifting-off, as perceived by investors.

Figure 8 presents the time series of both physical and risk-neutral ELB probabilities for maturities of 1 and 5 years. I translate these differences into the risk premium estimates using Equation (20) and represent them on the bottom-left panel. While it

Figure 8: Physical and risk-neutral ELB probabilities

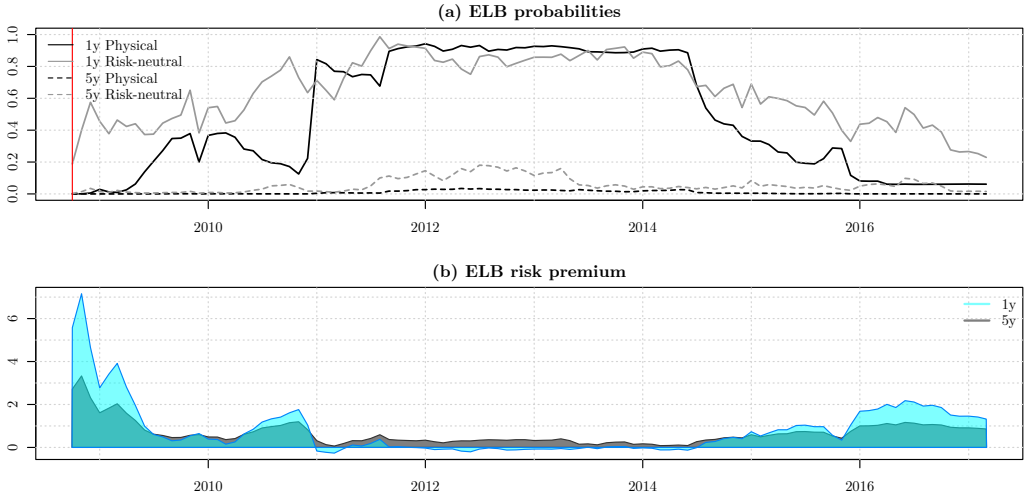

Notes: On panel (a), $\mathbb{P}$- and $\mathbb{Q}$-probabilities are respectively represented with black and grey lines, solid for 1y and dashed for 5y. Panel (b) presents the ELB risk premium as defined by Equation (20), blue for 1y and grey for 5y. All quantities are computed before applying corrections on the factors. The red vertical bar delimits the beginning of the ELB period.

starts largely positive, the 1y ELB risk premium becomes slightly negative from 2011 onwards until the beginning of 2015, indicating that investors fear that the central bank will be lifting off in the near future. After 2015, the ELB premium becomes positive again, showing that investors would prefer staying away from the lower bound. Interestingly, The ELB premium becomes positive in early 2015 while the actual liftoff was performed in December 2015. At the time, investors were arguing for an increase in interest rates while the Fed was waiting for further decreases in unemployment.[15] The magnitude is overall comparable to what is found in the credit risk literature comparing risk-neutral and physical default probabilities of entities (Driessen (2004) finds a log-ratio of 0.75 for corporates, and Monfort et al. (2021) find 1.5 for some European sovereigns).

Last, I dissect the ELB desirability into its different contributions and ask whether the embrace of the ELB is driven by the pricing of inflation components. To obtain the impact of the inflation trend, I recompute the counterfactual ELB Arrow-Debreu price after imposing that $\lambda_t^{(\pi^*)} = 0$. In the same fashion, I obtain the counterfactual price without inflation volatility pricing by restricting $\lambda_t^{(\sigma)} = 0$.[16] I obtain the contribution of each component by subtracting the obtained components from the baseline ELB risk premia.

I present the decomposition of the ELB risk premium at the 1y and 5y maturity on panels (a) and (b) of Figure 9, respectively. Two features emerge from the picture. First, the risk premium associated to inflation trend shocks always contribute negatively to the ELB risk premium, both for the 1y and 5y series and consistently throughout the ELB period. The magnitude is small nonetheless. Second, the pricing of inflation volatility shocks contributes negatively to the ELB risk premium before late 2011, and fluctuates around zero afterwards, with an order of magnitude bigger than the contribution of inflation trend. The effects are larger at the 5y horizon, par-

15. see for instance *"End Uncertainty over Fed rates liftoff"*, from the Financial Times dated November 3, 2015.

16. For both cases, I also impose that $\lambda_r = 0$ to avoid having pricing of inflation components through short-rate shocks.

Figure 9: Physical and risk-neutral ELB probabilities without inflation premia

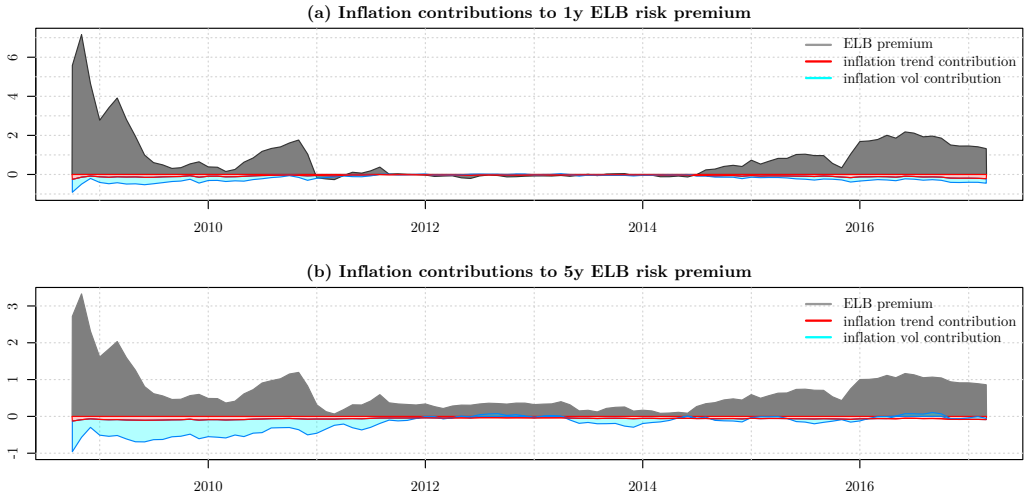

Notes: Both panels presents the ELB risk premium as defined by Equation (20). The red and blue components are the contributions of the inflation trend and volatility to the risk premium. Panel (a) and (b) present the results for the 1y and 5y maturities, respectively. All quantities are computed before applying corrections on the factors. The red vertical bar delimits the beginning of the ELB period.

ticularly for inflation volatility pricing, showing that the fear of inflation uncertainty contributes to the ELB desirability in the medium run, at least until the end of 2011.

5 Conclusion

In this paper, I investigate how asset prices can reveal information about inflation shocks during the ELB period. I provide a new way of modeling both nominal and real yield curves in an affine-quadratic framework, which allows for the presence of inflation trend and volatility and is consistent with a sticky lower bound on nominal yields. Relying on a combination of quadratic term structure models and the gamma-zero distribution, the QARG model is able to generate a short-term nominal rate stuck at the ELB for several periods. I show that the model provides closed-form formulas for nominal and real interest rates, interest rate forecasts, inflation forecasts, impulse-response functions, and probabilities to stay at the ELB under both physical and risk-neutral measure.

I provide empirical estimates of inflation components at the ELB using U.S. data. The ELB-consistent estimation combined with bond prices reveal that the ELB coincides with adverse inflation outcomes, i.e. persistently low inflation trend and high inflation volatility, supporting the view that inflation dynamics shifted at the ELB. These outcomes have a large influence on asset prices, and I show that they generate substantial long-run nominal term premia and short-run deflation fears that drive real yields upward. Second, I show that embracing the ELB is beneficial from the investors perspective, since the liftoff is considered as a bad state of the world. An impulse-response exercise reveals that lifting-off can create a wide variety of responses compared to normal times.

Acknowledgements

The author thanks Yakov Amihud, Daniel Andrei, Patrick Augustin, David Backus, Laurent Barras, Paul Beaumont, Sebastien Bétermier, Mikhail Chernov, Antonio Diez De Los Rios, Robert Engle, Andras Fulop, Bruno Feunou, Jean-Sébastien Fontaine, Xavier Gabaix, René Garcia, Joseph Haubrich, Leonardo Iania, Eric Mengus, Alain Monfort, Sarah Mouabbi, Fulvio Pegoraro, Florian Pelgrin, Eric Renault, Jean-Paul Renne, Glenn Rudebusch, Olivier Scaillet, Christopher Sims, Robert Whitelaw, Jonathan Wright. The author also thanks participants to the 7^{th} Bundesbank term structure workshop, 12^{th} ESWC conference in Montreal, the 9^{th} CFE international conference, 9^{th} annual SoFiE conference, Barcelona Graduate School of Economics Summer Forum in time series, 69^{th} Econometric society European summer meeting, 3^{rd} Econometric society European winter meeting, NYU-Stern QFE seminar, Brown University econometrics seminar, CREST financial econometrics seminar, Banque de France seminar, students' finance, macroeconomics and econometrics seminars at NYU, and students' finance seminar at Columbia.

6 Supplementary Material

The following is the Supplementary material related to this article.

References

Abrahams, M., T. Adrian, R. Crump, E. Moench, and R. Yu. 2016. "Decomposing Real and Nominal Yield Curve." *Journal of Monetary Economics.*

Adrian, T., and H. Wu. 2009. *The Term Structure of Inflation Expectations.* Staff Reports 362. Federal Reserve Bank of New York.

Ahn, D.-H., R. F. Dittmar, and A. R. Gallant. 2002. "Quadratic Term Structure Models: Theory and Evidence." *Review of Financial Studies* 15, no. 1 (March): 243–288.

Anderson, N., and J. Sleath. 2001. *New Estimates of the U.K. Real and Nominal Yield Curves.* Working Paper. Bank of England.

Andreasen, M., and A. Meldrum. 2011. *Likelihood Inference in Non-Linear Term Structure Models: The importance of the Zero Lower Bound.* Technical report.

———. 2015. *Market Beliefs about the UK Monetary Policy lift-off Horizon: A No-Arbitrage Shadow-Rate Term Structure Model Approach.* Technical report.

Andreasen, M., and A. Meldrum. 2018. "A Shadow Rate or a Quadratic Policy Rule? The Best Way to Enforce the Zero Lower Bound in the United States." *Journal of Financial and Quantitative Analysis.*

Andreasen, M. M., and B. J. Christensen. 2015. "The SR approach: A new estimation procedure for non-linear and non-Gaussian dynamic term structure models." *Journal of Econometrics* 184 (2): 420–451.

Ang, A., G. Bekaert, and M. Wei. 2008. "The Term Structure of Real Rates and Expected Inflation." *Journal of Finance* 63, no. 2 (April): 797–849.

Ang, A., J. Boivin, S. Dong, and R. Loo-Kung. 2011. "Monetary Policy Shifts and the Term Structure." *Review of Economic Studies* 78, no. 2 (February): 429–457.

Ang, A., and M. Piazzesi. 2003. "A No-Arbitrage Vector Autoregression of Term Structure Dynamics with Macroeconomic and Latent Variables." *Journal of Monetary Economics* 50, no. 4 (May): 745–787.

Aruoba, B., P. Cuba-Borda, and F. Schorfheide. 2017. "Macroeconomic Dynamics Near the ZLB: A Tale of Two Countries." *The Review of Economic Studies* 85, no. 1 (April): 87–118.

Backus, D. K., S. Foresi, and C. I. Telmer. 2001. "Affine Term Structure Models and the Forward Premium Anomaly." *Journal of Finance* 56, no. 1 (February): 279–304.

Bansal, R., and I. Shaliastovich. 2013. "A Long-Run Risks Explanation of Predictability Puzzles in Bond and Currency Markets." *The Review of Financial Studies* 26 (1): 1–33.

Barr, D., and J. Y. Campbell. 1997. "Inflation, Real Interest Rates, and the Bond Market: A Study of U.K. Nominal and Index-Linked Bond Prices." *Journal of Monetary Economics* 39:361–383.

Bauer, M. D., and G. D. Rudebusch. 2016. "Monetary Policy Expectations at the Zero Lower Bound." *Journal of Money, Credit and Banking.*

Bianchi, F., L. Melosi, and M. Rottner. 2021. "Hitting the Elusive Inflation Target." *Journal of Monetary Economics* 124:107–124.

Branger, N., C. Schlag, I. Shaliastovich, and D. Song. 2016. *Macroeconomic Bond Risks at the Zero Lower Bound.* Technical report.

Breach, T., S. D'amico, and A. Orphanides. 2020. "The Term Structure and Inflation Uncertainty." *Journal of Financial Economics* 138 (2): 388–414.

Camba-Mendez, G., and T. Werner. 2017. *The Inflation Risk Premium in the Post-Lehman Period.* Technical report. ECB.

Campbell, J. Y., A. Sunderam, and L. M. Viceira. 2017. "Inflation Bets or Deflation Hedges? The Changing Risk of Nominal Bonds." *Critical Finance Review,* no. 6, 263–301.

Carriero, A., S. Mouabbi, and E. Vangelista. 2018. "UK Term Structure Decompositions at the Zero Lower Bound." *Journal of Applied Econometrics* 33 (5): 643–661.

Chernov, M., and P. Mueller. 2012. "The Term Structure of Inflation Expectations." *Journal of Financial Economics,* no. 106, 367–394.

Christensen, J. H., and G. Rudebusch. 2015. "Estimating Shadow-Rate Term Structure Models with Near-Zero Yields." *Journal of Financial Econometrics* 13 (2): 226–259.

Christensen, J. H. E., and J. M. Gillan. 2012. *Could the U.S. Treasury Benefit from Issuing More TIPS.* Technical report. Federal Reserve Bank of San Francisco.

Christiano, L. 2017. *Comment on Cochrane, "Michelson-Morley, Fisher and Occam: The Radical Implications of Stable Quiet Inflation at the Zero Bound".* Technical report. Northwestern University.

Cochrane, J. H. 2017. "Michelson-Morley, Fisher, and Occam: The Radical Implications of Stable Quiet Inflation at the Zero Bound." In *NBER Macroeconomics Annual 2017, volume 32,* by M. Eichenbaum and J. A. Parker, 113–226. University of Chicago Press, June.

Cogley, T., G. Primiceri, and T. Sargent. 2010. "Inflation-Gap Persistence in the U.S." *American Economic Journal: Macroeconomics* 2, no. 1 (January): 43–69.

Coibon, O., and Y. Gorodnichenko. 2011. "Monetary Policy, Trend Inflation and the Great Moderation: An alternative Interpretation." *American Economic Review* 101:341–370.

D'Amico, S., D. H. Kim, and M. Wei. 2018. "Tips from TIPS: The Informational Content of Treasury Inflation-Protected Security Prices." *Journal of Financial and Quantitative Analysis* 53 (1): 395–436.

Dai, Q., and K. J. Singleton. 2002. "Expectation Puzzles, Time-varying Risk Premia, and Affine Models of the Term Structure." *Journal of Financial Economics* 63, no. 3 (March): 415–441.

Debortoli, D., J. Gali, and L. Gambetti. 2020. "On the Empirical (Ir)Relevance of the Zero Lower Bound Constraint." *NBER Macroeconomics Annual.*

Dittmar, R., A. Hsu, G. Roussellet, and P. Simasek. 2022. "Default Risk and the Pricing of U.S. Sovereign Bonds."

Driessen, J. 2004. "Is Default Event Risk Priced in Corporate Bonds?" *Review of Financial Studies.*

Duffee, G. R. 2002. "Term Premia and Interest Rate Forecasts in Affine Models." *Journal of Finance* 57 (1): 405–443.

Ehling, P., M. Gallmeyer, and C. Heyerdahl-Larsen. 2018. "Disagreement about inflation and the yield curve." *Journal of Financial Economics* 127:459–484.

Evans, M. D. D. 1998. "Real Rates, Expected Inflation and Inflation Risk Premia." *The Journal of Finance* 53, no. 1 (February).

Fernandez-Villaverde, J., and J. F. Rubio-Ramírez. 2007. "Estimating Macroeconomic Models: A Likelihood Approach." *Review of Economic Studies* 74 (4): 1059–1087.

Feunou, B., J. Fontaine, A. Le, and C. Lundblad. 2022. "Term Structure Modeling when Monetary Policy is Unconventional: A New Approach." *Management Science* 68 (11).

Feunou, B., and J.-S. Fontaine. 2014. "Non-Markov Gaussian Term Structure Models: The Case of Inflation." *Review of Finance* 18:1953–2001.

Filipovic, D., M. Larsson, and A. Trolle. 2017. "Linear-Rational Term Structure Models." *Journal of Finance* 72 (2): 655–704.

Fleckenstein, M., F. A. Longstaff, and H. Lustig. 2017. "Deflation Risk." *Review of Financial Studies* 30 (8): 2719–2760.

Fleckenstein, M., F. A. Longstaff, and H. Lustig. 2014. "The TIPS Treasury Bond Puzzle." *Journal of Finance* 69 (5): 2151–2197.

Gali, J. 2018. "The State of New Keynesian Economics: A Partial Assessment." *Journal of Economic Perspectives* 32 (3): 87–112.

Gourio, F., and P. Ngo. 2020. *Risk Premia at the ZLB: A Macroeconomic Interpretation.* Technical report. Chicago Fed.

Grischenko, O. V., and J.-Z. Huang. 2013. "The Inflation Bond Risk Premium: Evidence From the TIPS Market." *The Journal of Fixed Income.*

Gurkaynak, R. S., B. Sack, and J. H. Wright. 2007. "The U.S. Treasury yield curve: 1961 to the Present." *Journal of Monetary Economics* 54, no. 8 (November): 2291–2304.

———. 2010. "The TIPS Yield Curve and Inflation Compensation." *American Economic Journal: Macroeconomics* 2 (1): 70–92.

Haubrich, J., G. Pennacchi, and P. Ritchken. 2012. "Inflation Expectations, Real Rates, and Risk Premia: Evidence from Inflation Swaps." *Review of Financial Studies* 25 (5).

Imakubo, K., and J. Nakajima. 2015. "Estimating inflation risk premia from nominal and real yield curves using a shadow-rate model."

Joslin, S., M. Priebsch, and K. Singleton. 2014. "Risk Premiums in Dynamic Term Structure Models with Unspanned Macro Risks." *Journal of Finance* 69, no. 3 (June): 1197–1233.

Joslin, S., K. J. Singleton, and H. Zhu. 2011. "A New Perspective on Gaussian Dynamic Term Structure Models." *Review of Financial Studies* 24 (3): 926–970.

Kim, D. H., and A. Orphanides. 2012. "Term Structure Estimation with Survey Data on Interest Rate Forecasts." *Journal of Financial and Quantitative Analysis* 47, no. 01 (February): 241–272.

Kim, D. H., and M. Priebsch. 2013. *Estimation of Multi-Factor Shadow-Rate Term Structure Models.* Federal Reserve Board Discussion Paper Series. Federal Reserve Board.

Kim, D. H., and K. J. Singleton. 2012. "Term Structure Models and the Zero Bound: An Empirical Investigation of Japanese Yields." *Journal of Econometrics* 170 (1): 32–49.

King, T. 2019. "Expectation and Duration at the Effective Lower Bound." *Journal of Financial Economics* 134 (3): 736–760.

Kitsul, Y., and J. H. Wright. 2013. "The Economics of Options-Implied Inflation Probability Density Functions." *Journal of Financial Economics* 110 (3): 696–711.

Lansing, K. 2021. "Endogenous Forecast Switching Near the Zero Lower Bound." *Journal of Monetary Economics* 117:153–169.

Leippold, M., and L. Wu. 2007. "Design and Estimation of Multi-Currency Quadratic Models." *Review of Finance* 11, no. 2 (January): 167–207.

Lemke, W., and A. Vladu. 2016. *Below the zero lower bound – a shadow-rate term structure model for the euro area.* Technical report.

Mertens, T., and J. Williams. 2021. "What to Expect from the Lower Bound on Interest Rates: Evidence from Derivatives Prices." *American Economic Review* 111 (8).

Moench, E., and A. Vladu. 2018. *A Fine Term Structure Model for Real and Nominal Bonds.* Technical report. Bundesbank (mimeo).

Monfort, A., F. Pegoraro, J.-P. Renne, and G. Roussellet. 2017. "Staying at Zero with Affine Processes: A New Dynamic Term Structure Model." *Journal of Econometrics* 201 (2): 348–366.

———. 2021. "Affine Modeling of Credit Risk, Pricing of Credit Events and Contagion." *Management Science* 67 (6): 3321–3984.

Monfort, A., J.-P. Renne, and G. Roussellet. 2015. "A Quadratic Kalman Filter." *Journal of Econometrics* 187, no. 1 (July): 43–56.

Pericoli, M., and M. Taboga. 2015. *Understanding Policy Rates at the Zero Lower Bound: Insights from a Bayesian Shadow Rate Model.* Technical report. Bank of Italy.

Pflueger, C. E., and L. M. Viceira. 2016. "Handbook of Fixed Income Securities." Chap. Return Predictability in the Treasury Market: Real Rates, Inflation, and Liquidity (10), edited by P. Veronesi. Wiley.

Priebsch, M. 2013. *Computing Arbitrage-Free Yields in Multi-Factor Gaussian Shadow-Rate Term Structure Models.* Technical report. FRB.

Reichlin, L. 2015. *Commentary: Inflation During and After the Zero Lower Bound.* Technical report.

Renne, J.-P. 2014. "A Model of the Euro-Area Yield Curve with Discrete Policy Rates." *Studies in Nonlinear Dynamics and Econometrics* 21 (1).

Sack, B., and R. Elasser. 2004. *Treasury Inflation-Indexed Debt: A Review of the U.S. Experience.* Economic Policy Review. Federal Reserve Bank of New York, May.

Schupp, F. 2020. "The (ir)relevance of the nominal lower bound for real yield curve analysis."

Shen, P. 2006. *Liquidity Risk Premia and Breakeven Inflation Rates.* Economic Review. Federal Reserve Bank of Kansas City.

Swanson, E. T., and J. C. Williams. 2014. "Measuring the effect of the zero lower bound on Medium- and Longer-Term Interest Rates." *American Economic Review,* no. 104 (10): 3154–3185.

Williams, J. 2009. "Heeding Daedalus: Optimal Inflation and the Zero Lower Bound." *Brookings Papers on Economic Activity,* 1–37.

Wu, J. C., and F. D. Xia. 2016. "Measuring the Macroeconomic Impact of Monetary Policy at the Zero Lower Bound." *Journal of Money, Credit and Banking* 48 (2-3): 253–291.